

Multi-scale model suggests the trade-off between protein and ATP demand as a driver of metabolic changes during yeast replicative ageing

Barbara Schnitzer ^{*1,2}, Linnea Österberg ^{*1,2,3}, Iro Skopa ^{1,2}, Marija Cvijovic ^{1,2}

March 7, 2022

* These authors contributed equally

¹ Department of Mathematical Sciences, Chalmers University of Technology, Gothenburg, Sweden

² Department of Mathematical Sciences, University of Gothenburg, Gothenburg, Sweden

³ Department of Biology and Biological Engineering, Chalmers University of Technology, Gothenburg, Sweden

Corresponding Author: Marija Cvijovic, e-mail: marija.cvijovic@chalmers.se

1 Abstract

The accumulation of protein damage is one of the major drivers of replicative ageing, describing a cell's reduced ability to reproduce over time even under optimal conditions. Reactive oxygen and nitrogen species are precursors of protein damage and therefore tightly linked to ageing. At the same time, they are an inevitable by-product of the cell's metabolism. Cells are able to sense high levels of reactive oxygen and nitrogen species and can subsequently adapt their metabolism through gene regulation to slow down damage accumulation. However, the older or damaged a cell is the less flexibility it has to allocate enzymes across the metabolic network, forcing further adaptations in the metabolism. To investigate changes in the metabolism during replicative ageing, we developed a multi-scale mathematical model using budding yeast as a model organism. The model consists of three interconnected modules: a Boolean model of the signalling network, an enzyme-constrained flux balance model of the central carbon metabolism and a dynamic model of growth and protein damage accumulation with discrete cell divisions. The model can explain known features of replicative ageing, like average lifespan and increase in generation time during successive division, in yeast wildtype cells by a decreasing pool of functional enzymes and an increasing energy demand for maintenance. We further used the model to identify three consecutive metabolic phases, that a cell can undergo during its life, and their influence on the replicative potential, and proposed an intervention span for lifespan control.

1 Introduction

Cellular ageing is a complex multifactorial process affected by an intertwined network of effectors such as protein translation, protein quality control, mitochondrial dysfunction, and metabolism. Due to the conserved nature of hallmarks of ageing [1] unicellular organisms, such as the yeast *Saccharomyces cerevisiae*, have served as model organisms to gain deeper understanding of their synergistic effects and consequently mechanisms of ageing on a cellular level [2–4].

Loss of proteostasis is recognised as one of the hallmarks of replicative ageing [1, 5, 6], and is linked to the accumulation of damaged proteins over time [7, 8]. In yeast, a driving mechanism for the growing damage burden is the asymmetric distribution of damaged components between mother and daughter cell [8, 9]. An important precursor of protein damage is oxidative stress that is shown to increase with age [10–12] and is a byproduct of metabolic activity in the cells' mitochondria [12–15]. Reactive oxygen and nitrogen species

(ROS/RNS) are one of the most well-studied byproducts to which cells are constantly exposed even under normal conditions [16, 17]. The ability of cells to maintain protein homeostasis in response to intrinsic cellular and environmental factors, which accumulate over time, is one of the main determinants of lifespan [18]. Nutrient-sensing pathways are main contributors to the maintenance of the proteome during ageing. When inactivated, they affect a multitude of downstream processes, resulting in the cellular loss of proteostasis. Thus, they are one of the earliest events dictating ageing progression. To combat the loss of proteostasis associated with cellular ageing, cells have multiple stress-responsive mechanisms. For instance, Msn2 and Msn4, as general stress response proteins, as well as Yap1 and Skn7, as specific oxidative stress response proteins, are able to react to high levels of oxidative stress and can enhance the removal of ROS/RNS via adaptation of gene expression [19, 20]. Nevertheless, the accumulation of protein damage during replicative ageing cannot be prevented and in turn, affects the metabolism and its activity. It has been shown that cells to undergo distinct metabolic phases during their replicative life [21, 22], exhibiting a switch from energy production via fermentation to cellular respiration.

Hitherto, many mathematical models describing protein damage accumulation (reviewed in [23, 24]), signalling pathways (reviewed in [25, 26]) and metabolism [27] have been developed. Flux balance analysis (FBA) models have been extensively applied to predict fluxes through genome-scale reconstructions of metabolic networks of many different organisms and conditions [27–30]. In order to improve their predictive power, they have been extended by additional constraints, such as enzymatic and regulatory constraints [31–35] and lately proteome constraints [36]. Extensive and condition-specific regulatory constraints can be obtained by reconstructions of signalling pathways. Due to their size and availability of vast qualitative data, they are typically represented and simulated using logic or Boolean modelling [37–40]. Recent studies aimed at combining those two approaches into so-called hybrid modes, to understand the connection between signalling and the metabolism [35, 41]. However, most existing models are answering isolated questions regarding the cellular metabolism and its regulation with focus on short time scales compared to the lifespan of a cell. Further, they have not been used to understand damage accumulation over long time scales, i.e. ageing, despite the tight connection between the metabolism, ROS/RNS and damage accumulation. Recently, an FBA-based model was used to rationalise metabolic data at distinct time points during the replicative life of yeast cells [21]. While the study is based on the qualitative interpretation of the acquired data, mechanistic insights and dynamics are missing. On the other hand, dynamic models of protein damage accumulation have been applied to investigate replicative ageing on a single-cell level and the effect on the population level, however disregarding metabolic effects [42–45].

Taken together, while existing models have greatly improved our understanding of these key processes, they have also revealed gaps in the understanding of the complex interactions between them, as they are mainly studied individually and, in addition, lack both the complexity of the dynamics and the effects of the crosstalk between multiple components.

To overcome this gap, and to study the complex interplay and feedback between the metabolism and replicative ageing, in the context of damage accumulation and reactive oxygen species, we built a multi-scale model of yeast replicative ageing, that includes an enzyme-constrained FBA model, a Boolean model of nutrient signalling pathways and dynamic model of protein damage accumulation and cell growth. The model can simulate the lifespan of a cell being controlled by the metabolism, allowing to explore metabolic changes as the cell ages and becomes exposed to oxidative stress and protein damage.

2 Results

Construction of a multi-scale yeast replicative ageing model

To elucidate how nutrient and stress signalling, metabolism and protein damage accumulation influence and regulate each other during the life of a cell, we developed a multi-scale model of yeast replicative ageing (yMSA). The model consists of three interconnected modules: a Boolean model of the signalling network, an enzyme-constrained flux balance model of the central carbon metabolism and a dynamic model of growth and protein damage accumulation with discrete cell divisions (Fig 1, Table 1).

The first step in the construction was to extend a hybrid model of the central carbon metabolism and nutrient

79 signalling in budding yeast [35] by reactions and components attributed to the production and removal of
80 ROS and RNS, as well as the signalling response to it. In particular, we built a Boolean model of the Yap1
81 and Sln1 pathways (Fig 1A) and incorporated it in the already existing Boolean model of the nutrient sensing
82 pathways PKA, Snf1 and TOR [35]. While Msn2 and Msn4 are part of the PKA pathway, we also included
83 the crosstalk to the Yap1 pathway. In addition, we summarised reactions that create and remove ROS/RNS
84 (Fig 1B) and added them to the existing model of the central carbon metabolism [35]. The modules of
85 signalling and metabolism are connected by a transcriptional layer, that modifies the enzyme consumption
86 in the metabolic model depending on the binary activities of transcription factors in the Boolean model by
87 imposing regulatory constraints. In turn, the optimal fluxes of the enzyme constrained FBA (ecFBA) model
88 determine the states of input components in the Boolean model.

89 To validate the extensions, we demonstrated that the steady-state activity of the transcription factors in
90 the Boolean model is consistent with the presence or absence of oxidative stress (Fig S1). In addition,
91 we confirmed that the included production, sensing and removal of oxidative stress in the metabolic and
92 signalling network does not affect the exchange fluxes measured in a chemostat experiment [46], a widely
93 used experiment to validate metabolic models (Fig S2).

94 In the second step, we connected the described regulated ecFBA model to an ordinary differential equations
95 (ODE) model of cell growth and protein damage accumulation with discrete cell divisions (Fig 1C). Here,
96 the parameters of the ODE model depend on the optimal fluxes through the regulated ecFBA model. After
97 solving the ODE for one time step given those parameters, the resulting fraction of intact and damaged
98 proteins constrain the regulated ecFBA model for the next time step.

99 To simulate the whole lifespan of a cell, the model was iterated over time steps. Cell death automatically
100 occurs when the ecFBA becomes infeasible, caused by a too high protein damage burden such that the cell
101 is not able to generate enough energy for maintenance and growth anymore. Each time step is based on the
102 assumption that the signalling and metabolic adaptations happen on a much faster time scale than damage
103 accumulation and ageing. We furthermore accounted for a delay between an actual signalling event and its
104 effect on the metabolism through gene expression by applying the regulation step only after n_{delay} time steps.
105 All mathematical and computational details of each individual module as well as the crucial interfaces can
106 be found in the Methods section and in Text S1 and S2.

| Module | Type | Total number |
|---------------------|-------------------|--------------|
| Signalling network | components | 86 |
| | rules | 122 |
| Metabolic network | components | 138 |
| | enzymes | 140 |
| | fluxes | 375 |
| Damage accumulation | components/states | 3 |
| yMSA | components | 367 |
| | rules | 122 |
| | fluxes | 375 |

Table 1: Size of the individual modules and the yeast multi-scale model of ageing (yMSA).

107 The model predicts features of replicative ageing with distinct metabolic phases

108 To validate our multi-scale model, we tested if it can reproduce features of replicative ageing in yeast cells.
109 We focused firstly on the number of divisions (replicative lifespan) and the time between divisions (generation
110 time), and secondly on metabolic paths cells use to gain energy in the course of damage accumulation.

111 In each simulation, we started with a damage-free cell and let the model evolve over time until cell death
112 occurs. The objective of the metabolic model is always maximal growth, but a certain flexibility is allowed
113 to be able to reallocate enzymes when regulating.

114 Given the signalling and metabolic networks, we tested the effect of the ODE model parameters (non-
115 metabolic damage formation f_0 and damage repair r_0) on the lifespan. Our model predicts replicative
116 lifespans between 17-32 cell divisions in the tested parameter regime (Fig 2A), in accordance with measured
117 yeast wildtype lifespans of on average around 23 divisions [47–49]. The slower damage forms, the higher is the
118 replicative potential of the cell. An increase in the repair rate has a positive effect on the lifespan, however
119 it cannot counteract the large increase of dysfunctional proteins in mother cells caused by the asymmetric
120 damage segregation at cell division, being a major driver of replicative ageing [8, 9, 50, 51]. Only if repair
121 rates are more than approximately one order of magnitude higher than non-metabolic formation rates the
122 damage burden of retention can be overcome (Fig S3D).

123 To illustrate the dynamics of the model's components, we selected a representative wildtype cell with 23
124 divisions and an average generation time of around 1.5 hours and followed the optimal fluxes through the
125 metabolic network, the signals that the cell senses and its protein composition over time (Fig 2B). A typical
126 *in silico* cell starts with a fully functional protein pool that mediates chemical reactions in the metabolic
127 network. The resources can be fully exploited and allow for high growth and cell division rates. Over time,
128 as damage accumulates, the functional pool shrinks continuously, passing a point when the cell needs to
129 decrease the growth rate and metabolic fluxes have to be redistributed. Along with an increasing demand of
130 ATP for repairing damage, the cell needs to become more efficient in the ATP production. While most energy
131 during the maximal growth phase is produced via fermentation (high production of ethanol), respiration gets
132 more and more prominent when the growth rate drops (increase in oxygen O_2 uptake and acetate and carbon
133 dioxide CO_2 production). Consequently, damage is increasingly produced by ROS/RNS and the cell signals
134 oxidative stress, followed by an increased use of enzymes that are needed to remove those again. Older cells
135 with low growth rates produce less damage, and stress signalling is not active anymore. Instead, cells take
136 in less nutrients and eventually signal glucose limiting conditions. That old cells show signatures of starved
137 cells was recently confirmed experimentally [52]. Close to death, cells also take in ethanol to produce energy
138 and prolong lifespan. However, they can only grow slowly (Fig 2B).

139 Decreasing growth rates in our model induces slower generation times, i.e. times between cell divisions. In
140 particular, the last few divisions before cell death last significantly longer, as observed previously [48, 53].
141 In contrast to published models of protein damage accumulation that have to assume this decline in growth
142 [44, 45], here it is a direct output of the model.

143 Taken together, our model can reproduce characteristics of replicative ageing in wildtype yeast cells, being
144 a consequence of a shrinking pool of functional proteins available for the metabolism and an increasing
145 demand of energy for non-growth associated maintenance such as damage repair. In particular, simulated
146 cells undergo distinct metabolic phases: (I) maximal growth phase mainly mediated by fermentation, (II)
147 switching phase to respiration characterised by a mixed metabolism, a decrease in growth rate and an increase
148 in ROS/RNS production, and (III) slow growth phase defined by ethanol uptake (Fig 2D).

149 **Metabolic regulation by the signalling network is beneficial for the replicative** 150 **lifespan**

151 To identify the effect of stress signalling on the replicative lifespan, we simulated cells with varying regulation
152 strengths. By regulation strength we mean the magnitude of the constraints on the protein abundance caused
153 by stress signalling affecting the metabolic model. The regulation strength is different for every protein
154 depending on the solution space, and is controlled by a global regulation factor ϵ , as specified in Eq (1).
155 The model showed that increasing the strength of the regulation of enzymes is beneficial for the replicative
156 lifespan up to $\epsilon \approx 0.04$ (Fig 2C, 3A), corresponding to constraining a down- or upregulated enzyme in its
157 usage from above or below respectively by 4% of its enzyme variability. Wildtype cells, i.e. cell with around
158 23 divisions and an average generation time of 1.5 to 2h, can only be generated with this maximal regulation
159 strength and low damage formation rates (Fig 2C, Fig S3B). We observed that regulation has a particularly
160 strong effect on the maximal growth phase, i.e. phase I. Due to regulation the amount of damage that is
161 produced in this phase is reduced while the amount of divisions increased (Fig 3A, Fig S3C). An increase
162 in the number of divisions in phase II is only possible for a large impact of regulation on the metabolism
163 ($\epsilon > 0.02$). There is a similar maximal amount of damage that a cell can tolerate (damage at end of phase
164 III) regardless of the regulation, indicating that a decreased damage accumulation in the early life of the cell
165 is essential for the replicative lifespan.

166 The model cannot handle higher regulation factors than $\epsilon = 0.05$. If enzymes are too heavily constrained, i.e.
167 ϵ is large, the model sooner or later becomes over-constrained and infeasible only because of the regulation,
168 observed in a drop in time spent in respective phases (Fig 3A). The higher the regulation factor, the earlier
169 the drop occurs. We therefore restricted all following analysis to $\epsilon = 0.04$.

170 To further understand the impact of regulation in our model, we performed knockout experiments of key
171 proteins in the signalling pathways Snf1, PKA, TOR, Yap1 and Sln1, and combinations that are known from
172 literature to modulate lifespan (Fig 3B). The model qualitatively predicts a lifespan increase for deletion of
173 Msn2/4 and Rim15 while deletion of Msn2/4 alone decreases the lifespan [54]. Deletion of the TOR pathway
174 by inhibiting the TOR complex increases the lifespan [55]. Our model can however not predict lifespan
175 extension by Sch9 deletion [55], being an important cross-talk protein in the included pathways. While the
176 oxidative stress response proteins Yap1, Skn7 and Msn2/4 cannot modulate lifespan if deleted alone, only
177 the triple deletion reduces the lifespan, indicating a robustness of the cellular response to stress. Other
178 tested deletions, including the knockout of the PKA pathway, do not have an influence on the lifespan, but
179 potentially change the growth behaviour and consequently the cells' average generation times in our model.
180 In addition, the knockout experiments showed that the increase in the lifespan is in all cases due to a larger
181 number of divisions in phase I, while a reduction in the lifespan is often caused by fewer divisions in phase
182 II compared to the wildtype (Fig S4).

183 **An increased ATP demand for damage repair during ageing can explain the** 184 **switch from fermentation to respiration**

185 Our model emphasised that the maximal growth phase I is particularly important for the replicative life of a
186 cell. However, a cell cannot maintain that state forever since the pool of functional proteins decreases over
187 time, eventually leading to a drop in the growth rate and an increase in the protein damage. To understand
188 why cells at that point start switching from fermentation to respiration, we asked if it could be explained
189 by an increased energy (ATP) demand while ageing, i.e. a non-growth associated maintenance (NGAM).
190 We considered protein damage repair as one crucial type of NGAM, and therefore modelled $NGAM(t)$
191 to be linearly dependent on the fraction of damaged components $D(t)$ in the cell (Eq (5)), reaching its
192 maximal value $NGAM_{max}$ when the cell has a fully damaged proteome. We then simulated wildtype cells
193 with increasing $NGAM_{max}$ to evaluate the effect of the added ATP cost on the metabolic phases.

194 Our model demonstrated that the growth rate drops regardless of the additional ATP cost and cells enter
195 phase II and III. However, without NGAM ($NGAM_{max} = 0$), cells only ferment at lower rates, and do not
196 switch to a predominantly respiratory energy metabolism (Fig 3C). Only for larger $NGAM_{max}$, cells make
197 increasingly use of O_2 and produce CO_2 , indicating respiratory activity. Furthermore, phase III is only
198 reached with a non-zero $NGAM_{max}$.

199 Moreover, we observed that NGAM affects the damage tolerance of the cells, measured by the fraction of
200 damage in old cells at cell death (Fig 3D). It can be explained by the higher energy demand associated to
201 NGAM, which the cells can at some point during ageing not satisfy anymore given the metabolic network
202 and the resources. As a consequence, cell death is induced earlier. Only for $NGAM = 0$, the *in silico* cells
203 can be solved until it has a fully damaged proteome (here $\sim 0.46 g(gDW)^{-1}$ [56]), being however biologically
204 unreasonable.

205 In accordance with the value used in the yeast consensus model [27], we picked $NGAM_{max} = 0.7 [mmol(gDWh)^{-1}]$
206 in other simulations, leading to a damage tolerance of about half of the proteome in our model.

207 **Lifespan can be modulated by intervention in specific metabolic phases**

208 Next, we asked if it is possible to control lifespan in our model by enhancing or repressing the right processes
209 in the right moment. We performed deletions and overexpressions of all enzymes, as well as of combinations
210 of isoenzymes that catalyse the same reaction, and analysed the resulting replicative lifespans compared to
211 the wildtype (Fig 4A-B, File S1). All simulations were performed for the respective perturbation during
212 the whole life, only in phase I, only in phase II and only in phase III. Deletion in the model corresponds to
213 restricting the usage of the enzyme(s) to 0. In contrast, overexpression is modelled by constraining the usage
214 of the enzyme(s) to 150% of the optimal usage after the regulation step.

215 In both cases the enzyme perturbation can generate non-dividing cells (not necessarily non-viable but possibly
216 growing at very low growth rates), if the enzyme is perturbed over the whole life or only in phase I. Generally,
217 we observed that deletions are in our model the harsher intervention, and can often be more disadvantageous
218 for the number of divisions in the respective phases. This can be partly explained by the fact that the
219 metabolic model is limited to the central carbon metabolism and many of the reactions are crucial for the
220 functioning of the cell.

221 However, a perturbation can also cause an increase in the replicative lifespan. Interestingly, cells can divide
222 more often if the enzyme is perturbed only in one specific phase. Those enzymes do not necessarily
223 coincide with enzymes that increase lifespan in the case of perturbation during the whole lifespan. This can
224 happen because an enzyme that is beneficial for the lifespan in one metabolic phase can at the same time be
225 disadvantageous in another phase. Examples for that are particular overexpressions in phase I (Fig 4A) and
226 particular deletions in phase I and II (Fig 4B), that do not appear to be beneficial if perturbed over the whole
227 lifespan. Since phase III is in general the shortest and least important in replicative ageing, as well as not all
228 cells reach that phase, we did not observe large differences between perturbations in that phase compared to
229 the wildtype.

230 **Enzyme perturbations can enforce metabolic adaptations during replicative ageing**

231 To gain further insight on how those enzyme perturbations affect the replicative lifespan, we studied the
232 changes in the cumulative enzyme usage compared to the wildtype. We further looked for patterns between
233 enzyme usages, related pathways and effects on the number of divisions (Fig 4C-D and Fig S5). The data
234 that the following results are based on can be found in detail in File S1.

235 A perturbation of an enzyme can naturally result in an increase or decrease in the enzyme usage compared to
236 the wildtype. Here, we showed that both can have a similar effect on the replicative lifespan of the cell. An
237 increase in the lifespan can be induced by an increased usage of an enzyme, likely by enhancing processes that
238 are beneficial for the number of divisions. On the other hand, a similar increase in the lifespan can arise from
239 using less of a certain enzyme, indicating that high usage of this enzyme is disruptive for certain processes
240 that correlate with lifespan. Interestingly, we found cases where an overexpression leads to a decreased usage
241 (Fig 4C, marked with TCA cycle) and a deletion can result in an increased usage (Fig 4D, marked with
242 glycolysis) of the enzyme in relation to the wildtype, showing that cells compensate for the loss or overuse
243 in the successive metabolic phases, caused by altered preconditions.

244 To study more closely how the cells adapt to the perturbations (File S1), several scenarios have been tested.
245 We found that prolonging the time spent in phase I, can result in an increase of cell divisions. A prolongation
246 of phase I can be reached by overexpressing particular enzymes from the oxidative phosphorylation pathway
247 in phase I, or by deleting particular enzymes in the glycolysis in phase I. More specifically, we found that
248 those enzymes typically shorten lifespan instead when overexpressed over the whole lifespan (Fig S5A, e.g.
249 NDI1, TIM11, OLI1, several ATPs, and Fig S5B, e.g. PGI1, TPI1).

250 Another possibility to increase lifespan is enhancing certain enzymes that remove ROS/RNS, being benefi-
251 cial in both phase I and II. Similarly, overexpressing particular enzymes in the TCA cycle can as well be
252 advantageous in those two phases. Effectively, all cases described so far lead to a decreased growth rate that
253 is responsible for an increase in lifespan. It is a consequence of forcing a bit of respiration already in phase
254 I. In addition, supporting a faster switch from phase II to III can lead to more cell divisions, for instance by
255 deleting specific enzymes in the oxidative phosphorylation in phase II. In those cases, phase III is prolonged
256 instead. Also here, the respective enzymes are typically only beneficial for the lifespan when deleted in phase
257 II but not over the whole lifespan (Fig S5B, e.g. PGI1, TPI1).

258 **Enzymes responsible for removing hydrogen peroxide affect lifespan**

259 Lastly, we investigated in more detail how sensitive the lifespan is to changes in the enzymes added for
260 ROS/RNS production and removal (Fig S5B). We found that the system is in general robust towards per-
261 turbations in those enzymes. Most perturbations do not affect the lifespan, with few exceptions [57]. Double
262 deletion of Trx1 and Trx2 or the deletion of Trr1, enzymes that involved in the transformation from H₂O₂ to
263 water, are harmful for cell growth and divisions in all three phases [58]. Double deletion of Sod1 and Sod2,
264 enzymes that create hydrogen peroxide or superoxide, show similar behaviour [57]. Further, we observed that

265 overexpression of Sod1, Sod1 and Sod2, Gpx3, and Glr1 completely or in phase II surprisingly reduce the
266 replicative lifespan of the cell [54]. In contrast, overexpression of Trx1, Trx1 and Trx2 and Trx1 in the same
267 phases increase lifespan, likely by enhancing removal of reactive oxidative species efficiently.

268 3 Discussion

269 Here, we presented a novel multi-scale model consisting of the metabolism, stress signalling and damage
270 accumulation in the budding yeast *S. cerevisiae* that allowed us to study key features of replicative ageing.
271 We incorporated reactive oxygen and nitrogen species (ROS and RNS), as a crucial interface between the
272 metabolism and ageing, and accounted for the asymmetric damage segregation at cell division. The model
273 is based on established modelling techniques in Systems Biology, such as Boolean modelling, flux balance
274 analysis and ordinary differential equations, but stands out due to the combination of the three modules to a
275 larger interconnected model (Table 1), that tackles the challenge to deal with the complexity and multi-scale
276 nature of ageing. Our model could reproduce realistic values for both the replicative lifespans and generation
277 times of yeast wildtype cells, as characterised by experiments. We further showed that a regulatory layer
278 is crucial for replicating wildtype cells in our model. Previously proposed metabolic phases [21, 22] are a
279 direct outcome of our model, and here we demonstrated that those phases are tightly linked to the replicative
280 lifespan using enzyme overexpressions and deletions.

281 We identified the non-growth associated maintenance (NGAM) as a key feature of the metabolic phases.
282 Traditionally, NGAM is defined as the substrate yield that is used for other processes than growth [59–62].
283 NGAM is a dynamic variable, highly dependent on for instance the metabolic state of the cell or the nutrient
284 composition in the media. However, there is a lack of consensus in what is included in the NGAM, since
285 there are no direct ways to experimentally assess and quantify ATP demands specific to certain processes.
286 Here, we assumed that protein repair and replacement of damaged proteins with functioning proteins are the
287 main contributions to the NGAM, such that the NGAM should scale with protein damage. In the model,
288 NGAM is defined to be linearly dependent on the damaged protein fraction, which increases with age. This
289 simplified age-dependent definition provides a new perspective on the cost, based on the idea that the more
290 damage there is in a cell, the more energy it needs for repair and degradation.

291 We tested how sensitive the model is to the maximal value of NGAM, when damage levels are the highest,
292 and studied its effect on ageing phenotypes. We found that the increased ATP cost connected to the NGAM
293 has a major effect when lower enzyme availability causes a decrease in the growth rate, since in that moment
294 damage accumulation starts to increase in speed. More specifically, the NGAM changes the dynamics of the
295 switch from fermentation to respiration happening in phase II. Leupold et al. [21] speculated that an increase
296 in cellular volume and thus a decreased volumetric substrate intake lead to the switch of metabolic phenotype
297 by inhibiting the carbon uptake rate [63]. In our model, NGAM plays a crucial role in determining the ratio
298 between respiration and fermentation in the mixed metabolism that characterises phase II, and the model
299 showed that without NGAM the switch is not induced properly, but fermentation is mainly slowed down.
300 Since cellular respiration has a higher ATP yield compared to fermentation, we propose that an increased
301 ATP demand due to a non-zero NGAM together with a decreasing capacity to take up nutrients is another
302 explanation for the metabolic switch during replicative ageing.

303
304 Gene regulation is a crucial mechanism to adapt to stressful conditions and to ensure that the right proteins
305 are expressed in the proper time. In our model, regulation acts upon internal stress caused by ageing. It
306 helps to increase the replicative lifespan, even under nutrient rich conditions without artificial stress, by
307 inhibiting damage formation predominantly in phase I, but also in phase II. Delaying the onset of protein
308 damage accumulation further prolongs the cell’s health span, and in that way has a positive effect on the
309 progeny and thus the whole cell population [45]. The model demonstrated that regulatory constraints are an
310 important extension of FBA models in the context of ageing, as they are key in predicting wildtype lifespans.
311 Regulation and stress have been extensively studied in relation to replicative ageing [64–66]. Gene modi-
312 fications of proteins in the nutrient and stress signalling systems, such as Msn2/4 and Tor1/2, have been
313 connected to longevity [64], and our model was able to qualitatively predict long- or short-lived mutants for
314 some gene knockouts. Similarly, we simulated perturbations in the enzymes contained metabolic model, and
315 were able to confirm some qualitative correlations between enzyme deletion or overexpression and lifespan,

316 focusing on enzymes connected to ROS/RNS. Nonetheless, the model cannot capture all known relations.
317 There are both technical reasons and knowledge gaps that could cause the discrepancies when comparing
318 the model to an observed phenotype. Firstly, connecting transcription factor activity to changes in gene
319 expression is a non-trivial problem. Advanced methods utilising high-throughput data can provide means to
320 improve the connection between signalling and the metabolism, estimating probabilistic mappings between
321 transcription factor activities and gene expression, and translating those to the metabolic fluxes [41, 67].
322 However, those models are non-mechanistic and highly context-dependent, and the ability to extrapolate to
323 other conditions, where data is limited, is questionable. Secondly, the topology of the signalling network is
324 not completely elucidated and there are still conditions under which we cannot explain responses given our
325 current knowledge [25, 40]. Moreover, by implementing signalling as a Boolean model, we reduced the com-
326 plexity of the system which automatically limits the complexity of the model responses. Lastly, even though
327 FBA models are good in predicting exchange fluxes and qualitative changes in pathway fluxes, individual
328 enzyme predictions remain a challenge [35].

329
330 Motivated by the distinct metabolic phases a cell undergoes during ageing, we propose an intervention span
331 for lifespan control. Our model showed that an enzyme perturbation in a specific phase can prolong lifespan,
332 while the same perturbation over the whole lifespan can shorten lifespan. The same thought can be reversed,
333 and such models can help to identify enzymes that shorten lifespan when perturbed in a specific metabolic
334 phase, but do not affect or even prolong lifespan when perturbed over the whole life. While we focused
335 solely on lifespan extensions in the context of ageing, phase-dependent interventions using our modelling
336 approach can have further applications. Phase I is dominated by fermentation, and genetic modifications
337 that prolong this phase can be of great interest in industrial applications to increase production yields. For
338 this purpose, replacing the reconstruction of the central carbon metabolism by a reconstruction of the yeast
339 consensus metabolic network [27] together with the addition of relevant production pathways can extend the
340 applicability of our model and enables testing of a greater variety of interventions.
341 Practically, to realise such a phase-specific intervention, inducible and conditionally expressed genes in
342 genetically modified production strains have established experimental methods.

343 Mathematical modelling typically is a balance between biological realism and mathematical simplicity, such
344 that also our model is naturally based on numerous assumptions and simplifications. Yet, the model we
345 constructed constitutes a first attempt to shed light on replicative ageing from a multi-scale perspective,
346 incorporating several hallmarks of ageing. We could replicate important features of replicative ageing, and
347 moved a step further in understanding and utilising the connection between the metabolism and ageing.
348 Moreover, the modularity of our approach facilitates developing and extending the model further, and trans-
349 lating it to other organisms. Multi-scale mathematical models, like the one presented here, are an important
350 aid to bridge the gap between biological realism, the knowledge we have and experimental feasibility, and to
351 test hypotheses in a complex phenomenon like ageing.

352 4 Methods

353 **Extension of a regulated enzyme-constrained metabolic model by production of** 354 **reactive oxygen and nitrogen species and the cellular response to them**

355 We based our work on a previously published hybrid model of nutrient signalling and the metabolic network
356 of the central carbon metabolism, that consists of a Boolean modelling approach of the nutrient signalling
357 pathways TOR, PKA and Snf1 combined with an enzyme-constrained flux balance analysis approach (ecFBA)
358 via a transcriptional layer [35]. In this model, the first step is to optimise the ecFBA model for a given
359 objective. The optimal glucose uptake flux then determines the state of glucose in the Boolean model, i.e.
360 glucose is present if the glucose intake exceeds a critical threshold glc_c^{in} . A switch of the state induces a
361 cascade of events in the Boolean model and eventually its steady state gives rise to which of the transcription
362 factors in the pathways are active. For each transcription factor in the Boolean model the database Yeasttract
363 [68] can tell which genes are subsequently expressed or inhibited. Since also enzymes of the ecFBA model
364 are included in the target lists from Yeasttract the constraints on their usages in the ecFBA model can be
365 altered accordingly.

366 In particular, for each enzyme i a rank based on the number of transcription factors that up- or down-regulate
 367 it determines if the netto regulation is positive or negative. The bounds of the enzymes $e_{i,min}$ and $e_{i,max}$ in
 368 the ecFBA are then constraint according to:

$$\begin{aligned} \text{upregulation :} & \quad e_{i,min} \leftarrow e_{i,min} + \Delta_i \cdot \epsilon \\ \text{downregulation :} & \quad e_{i,max} \leftarrow e_{i,max} - \Delta_i \cdot \epsilon, \end{aligned} \tag{1}$$

369 with ϵ being a regulation factor, and Δ_i being the range of enzyme usages that the model can take (result
 370 from enzyme variability analysis) without varying the objective value of the original optimisation up to some
 371 flexibility. The solution of the ecFBA with the new constraints corresponds to the regulated metabolic
 372 network.

373 We used the same methodology but increased the size of the metabolic network by including reactions in
 374 the ecFBA that produce and remove reactive oxygen (ROS) and nitrogen (RNS) species (Fig 1A). The
 375 major source are electrons that escape from the electron transport chain in the mitochondria during cellular
 376 respiration [15] and react with oxygen to produce superoxide. Superoxide can via RNS be transformed to
 377 hydroxyl radicals which can oxidise and thus damage proteins. A second way to create protein damage from
 378 superoxide is via hydrogen peroxide. Hydrogen peroxide in the model is either removed or reacts further to
 379 become the dangerous hydroxyl radical [12, 16, 19, 20, 64, 69, 70]. Subsequently, certain levels of oxidative
 380 stress in the cell trigger stress signalling [19]. Therefore, we added the oxidative stress sensing pathways
 381 Yap1 and Sln1 to the Boolean model (Fig 1B), that induce regulation of the metabolic network via gene
 382 regulation by the transcription factors Yap1 and Skn7 [71–85]. To improve the transcriptional layer, we
 383 extended the data from Yeabstract by data from [86], that particularly focused on the effects of Yap1 and
 384 Skn7. The presence of oxidative stress in the Boolean model is steered by the production of proteins with
 385 oxidative damage in the ecFBA model, that if larger than d^c switches the presence of H_2O_2 to 1. Similarly,
 386 the enzyme usage of Trx1/2, proteins known to regulate the Yap1 pathway as well as to activate Msn2/4,
 387 determines if the protein is present in the Boolean model, in particular if it exceeds a critical threshold trc^c .
 388 In total, we added 9 new components and 13 new rules to the existing model of nutrient signalling to account
 389 for oxidative stress signalling by the Yap1 and the Sln1 pathway. Moreover, the ecFBA model was extended
 390 by 53 new reactions and 41 new components including 13 new enzymes.

391 Multi-scale model construction of the regulated cellular metabolism and replica- 392 tive ageing

393 We used the extended regulated enzyme-constrained FBA model described above and optimised it for maximal
 394 growth and parsimony. Besides the resulting optimal value of the growth rate $g(t)$, the model now also outputs
 395 a protein damage formation rate $f_m(t)$ that is caused by oxidative stress.

396 To evaluate the protein damage formation over time, we incorporated a third module: a dynamical model
 397 based on a simple system of ordinary differential equations. The states are the cell’s dry weight $M(t)$, its
 398 fractional intact protein content $P(t)$ and its fractional damaged protein content $D(t)$. The latter two can
 399 be transformed between each other, however the total fraction of proteins $P(t) + D(t)$ is assumed to remain
 400 constant over time ($\Leftrightarrow \frac{d}{dt}(P(t) + D(t)) = 0$).

$$\frac{dM(t)}{dt} = g(t)M(t) \tag{2}$$

$$\frac{dP(t)}{dt} = -(f_m(t) + f_0)P(t) + r_0D(t) \tag{3}$$

$$\frac{dD(t)}{dt} = +(f_m(t) + f_0)P(t) - r_0D(t). \tag{4}$$

401 Besides the parameters that are directly obtained from the solution of the ecFBA, we included a non-metabolic
 402 damage formation rate f_0 to account for all other processes that produce damage, and a damage repair rate
 403 r_0 that represents all mechanisms that repair damaged proteins.

404 The solution of the ODE model (2)-(4) for a small time step determines the fraction of the enzyme pool that
 405 is available in the ecFBA model in the next time step. Moreover, an increasing amount of damage increases

406 the non-growth associated ATP cost (NGAM) in the ecFBA model, assuming that the cell needs to allocate
407 more energy to repair damage. In particular,

$$NGAM(t) = \frac{D(t)}{P(t) + D(t)} \cdot NGAM_{max}. \quad (5)$$

408 In this way, we can simulate ageing as the accumulation of damage in the cell over time. Consequently, the
409 amount of enzymes available in the ecFBA model shrinks, and the metabolic fluxes are forced to adapt in
410 the course of the cell's lifespan.

411 As soon as a cell has built up enough in biomass, $M(t_d) = s^{-1}M(0)$, it divides into a mother and a daughter
412 cell, according to a size proportion $s \in [0.5, 1]$ that corresponds to the fraction of biomass that remains in the
413 mother cell at cell division. While the total fraction of proteins is constant in both cell compartments, the
414 composition of functional and damaged proteins is determined by damage retention. The larger the retention
415 factor $re \in [0, 1]$, the more damage is retained in the mother cell. The states of mother and daughter cell are
416 updated according to

| | mother | daughter | (6) |
|-----|-------------------------------|--|-----|
| 417 | $M \leftarrow sM(t_d) = M(0)$ | $M \leftarrow (1 - s)M(t_d) = (1 - s)s^{-1}M(0)$ | |
| | $P \leftarrow (1 - re)P(t_d)$ | $P \leftarrow (1 + re)P(t_d)$ | |
| | $D \leftarrow (1 + re)D(t_d)$ | $D \leftarrow (1 - re)D(t_d)$ | |

418 Cell death occurs when the enzyme-constrained FBA becomes infeasible, i.e. when the cell is not able to
419 obtain enough energy for maintenance and growth anymore.

420 By including the dynamic module for damage accumulation, we incorporated the notion of time to the
421 regulated metabolic model, under the assumption that the steady state of the metabolism is reached fast in
422 the time scale of replicative ageing. It further led us to introduce a time delay between the moment the cell
423 receives a stress signal and the moment the metabolic network is affected by altered gene regulation.

424 A schematic view of the complete model is shown in Fig 1. All details about the individual models and the
425 extensions made in this work can be found in Text S1.

426 Simulation details

427 All simulations and their analysis were performed in the programming language Julia version 1.6 [87] and
428 were run on a normal computer with 2.3 GHz Dual-Core Intel Core i5 and 8GB RAM. The linear program
429 (ecFBA) was solved using the JuMP and Gurobi packages. The developed model can be downloaded from
430 <https://github.com/cvijoviclab/IntegratedModelMetabolismAgeing>. Model parameters, constraints
431 and pseudo code for a lifespan simulation can be found in Text S2.

432 Acknowledgements

433 This work was supported by the Swedish Research Council (VR2016-03744 and VR2017-05117) and the
434 Swedish Foundation for Strategic Research (FFL15-0238).

435 Competing interests

436 The authors declare no competing interests.

References

1. López-Otín, C., Blasco, M. A., Partridge, L., Serrano, M. & Kroemer, G. The Hallmarks of Aging. *Cell* **153**, 1194–1217 (June 2013).
2. Jazwinski, S. M. Growing Old: Metabolic Control and Yeast Aging. *Annu. Rev. Microbiol.* **56**, 769–792 (Oct. 2002).
3. Fontana, L., Partridge, L. & Longo, V. D. Extending Healthy Life Span—From Yeast to Humans. *Science* **328**, 321–326 (Apr. 2010).
4. Denoth Lippuner, A., Julou, T. & Barral, Y. Budding yeast as a model organism to study the effects of age. *FEMS Microbiol Rev* **38**, 300–325 (Mar. 2014).
5. Klaiaps, C. L., Jayaraj, G. G. & Hartl, F. U. Pathways of cellular proteostasis in aging and disease. *J Cell Biol* **217**, 51–63 (Jan. 2018).
6. Kaushik, S. & Cuervo, A. M. Proteostasis and aging. *Nat Med* **21**, 1406–1415 (Dec. 2015).
7. Levine, R. L. Carbonyl modified proteins in cellular regulation, aging, and disease. *Free Radical Biology and Medicine* **32**, 790–796 (May 2002).
8. Aguilaniu, H., Gustafsson, L., Rigoulet, M. & Nyström, T. Asymmetric Inheritance of Oxidatively Damaged Proteins During Cytokinesis. *Science* **299**, 1751–1753 (Mar. 2003).
9. Erjavec, N., Larsson, L., Grantham, J. & Nystrom, T. Accelerated aging and failure to segregate damaged proteins in Sir2 mutants can be suppressed by overproducing the protein aggregation-remodeling factor Hsp104p. *Genes & Development* **21**, 2410–2421 (Oct. 2007).
10. Cabiscol, E., Piulats, E., Echave, P., Herrero, E. & Ros, J. Oxidative Stress Promotes Specific Protein Damage in *Saccharomyces cerevisiae*. *Journal of Biological Chemistry* **275**, 27393–27398 (Sept. 2000).
11. Laun, P. *et al.* Aged mother cells of *Saccharomyces cerevisiae* show markers of oxidative stress and apoptosis: Aged yeast mother cells undergo apoptosis. *Molecular Microbiology* **39**, 1166–1173 (Feb. 2004).
12. Perrone, G. G., Tan, S.-X. & Dawes, I. W. Reactive oxygen species and yeast apoptosis. *Biochimica et Biophysica Acta (BBA) - Molecular Cell Research* **1783**, 1354–1368 (July 2008).
13. Wheeler, G. L. & Grant, C. M. Regulation of redox homeostasis in the yeast *Saccharomyces cerevisiae*. *Physiol Plant* **120**, 12–20 (Jan. 2004).
14. Nickel, A., Kohlhaas, M. & Maack, C. Mitochondrial reactive oxygen species production and elimination. *Journal of Molecular and Cellular Cardiology* **73**, 26–33 (Aug. 2014).
15. Zhao, R.-Z., Jiang, S., Zhang, L. & Yu, Z.-B. Mitochondrial electron transport chain, ROS generation and uncoupling. *Int J Mol Med* (May 2019).
16. Halliwell, B. *Active Oxygen in Biochemistry* (2012).
17. Halliwell, B. & Gutteridge, J. M. C. *Free Radicals in Biology and Medicine* 5th ed. (Oxford University Press, Oxford, 2015).
18. Morimoto, R. I. & Cuervo, A. M. Proteostasis and the Aging Proteome in Health and Disease. *The Journals of Gerontology Series A: Biological Sciences and Medical Sciences* **69**, S33–S38 (June 2014).
19. Temple, M. D., Perrone, G. G. & Dawes, I. W. Complex cellular responses to reactive oxygen species. *Trends in Cell Biology* **15**, 319–326 (June 2005).
20. Ayer, A., Gourlay, C. W. & Dawes, I. W. Cellular redox homeostasis, reactive oxygen species and replicative ageing in *Saccharomyces cerevisiae*. *FEMS Yeast Research* **14**, 60–72 (Feb. 2014).
21. Leupold, S. *et al.* *Saccharomyces cerevisiae* goes through distinct metabolic phases during its replicative lifespan. *eLife* **8**, e41046 (Apr. 2019).
22. Jacquet, B., Aspert, T., Laporte, D., Sagot, I. & Charvin, G. Monitoring single-cell dynamics of entry into quiescence during an unperturbed life cycle. *eLife* **10**, e73186 (Nov. 2021).
23. Santiago, E., Moreno, D. F. & Acar, M. Modeling aging and its impact on cellular function and organismal behavior. *Experimental Gerontology* **155**, 111577 (Nov. 2021).

24. Borgqvist, J., Dainese, R. & Cvijovic, M. *Systems Biology* 243–264 (Wiley-VCH Verlag GmbH & Co. KGaA, Weinheim, Germany, Mar. 2017).
25. Lubitz, T. *et al.* Network reconstruction and validation of the Snf1/AMPK pathway in baker's yeast based on a comprehensive literature review. *npj Syst Biol Appl* **1**, 15007 (Dec. 2015).
26. Persson, S., Shashkova, S., Österberg, L. & Cvijovic, M. Modelling of glucose repression signalling in yeast *Saccharomyces cerevisiae*. *FEMS Yeast Research*, foac012 (Mar. 2022).
27. Lu, H. *et al.* A consensus *S. cerevisiae* metabolic model Yeast8 and its ecosystem for comprehensively probing cellular metabolism. *Nat Commun* **10**, 3586 (Dec. 2019).
28. Duarte, N. C. *et al.* Global reconstruction of the human metabolic network based on genomic and bibliomic data. *Proceedings of the National Academy of Sciences* **104**, 1777–1782 (Feb. 2007).
29. Feist, A. M. & Palsson, B. O. The growing scope of applications of genome-scale metabolic reconstructions using *Escherichia coli*. *Nat Biotechnol* **26**, 659–667 (June 2008).
30. Oberhardt, M. A., Palsson, B. O. & Papin, J. A. Applications of genome-scale metabolic reconstructions. *Mol Syst Biol* **5**, 320 (Jan. 2009).
31. Sánchez, B. J. *et al.* Improving the phenotype predictions of a yeast genome-scale metabolic model by incorporating enzymatic constraints. *Mol Syst Biol* **13**, 935 (Aug. 2017).
32. Covert, M. W., Schilling, C. H. & Palsson, B. O. Regulation of Gene Expression in Flux Balance Models of Metabolism. *Journal of Theoretical Biology* **213**, 73–88 (Nov. 2001).
33. Covert, M. W. & Palsson, B. O. Transcriptional Regulation in Constraints-based Metabolic Models of *Escherichia coli*. *Journal of Biological Chemistry* **277**, 28058–28064 (Aug. 2002).
34. Marmiesse, L., Peyraud, R. & Cottret, L. FlexFlux: combining metabolic flux and regulatory network analyses. *BMC Syst Biol* **9**, 93 (Dec. 2015).
35. Österberg, L. *et al.* A novel yeast hybrid modeling framework integrating Boolean and enzyme-constrained networks enables exploration of the interplay between signaling and metabolism. *PLoS Comput Biol* **17**, e1008891 (Apr. 2021).
36. Elsemman, I. E. *et al.* Whole-cell modeling in yeast predicts compartment-specific proteome constraints that drive metabolic strategies. *Nat Commun* **13**, 801 (Dec. 2022).
37. Klamt, S., Saez-Rodriguez, J., Lindquist, J. A., Simeoni, L. & Gilles, E. D. A methodology for the structural and functional analysis of signaling and regulatory networks. *BMC Bioinformatics* **7**, 56 (2006).
38. Christensen, T. S., Oliveira, A. & Nielsen, J. Reconstruction and logical modeling of glucose repression signaling pathways in *Saccharomyces cerevisiae*. *BMC Syst Biol* **3**, 7 (2009).
39. Mori, T., Flöttmann, M., Krantz, M., Akutsu, T. & Klipp, E. Stochastic simulation of Boolean rxncon models: towards quantitative analysis of large signaling networks. *BMC Syst Biol* **9**, 45 (Dec. 2015).
40. Welkenhuysen, N., Schnitzer, B., Österberg, L. & Cvijovic, M. Robustness of Nutrient Signaling Is Maintained by Interconnectivity Between Signal Transduction Pathways. *Front. Physiol.* **9**, 1964 (Jan. 2019).
41. Niu, P. *et al.* TRIMER: Transcription Regulation Integrated with Metabolic Regulation. *iScience* **24**, 103218 (Nov. 2021).
42. Erjavec, N., Cvijovic, M., Klipp, E. & Nystrom, T. Selective benefits of damage partitioning in unicellular systems and its effects on aging. *Proceedings of the National Academy of Sciences* **105**, 18764–18769 (Dec. 2008).
43. Clegg, R. J., Dyson, R. J. & Kreft, J.-U. Repair rather than segregation of damage is the optimal unicellular aging strategy. *BMC Biol* **12**, 52 (Dec. 2014).
44. Borgqvist, J., Welkenhuysen, N. & Cvijovic, M. Synergistic effects of repair, resilience and retention of damage determine the conditions for replicative ageing. *Sci Rep* **10**, 1556 (Dec. 2020).

45. Schnitzer, B., Borgqvist, J. & Cvijovic, M. The synergy of damage repair and retention promotes rejuvenation and prolongs healthy lifespans in cell lineages. *PLoS Comput Biol* **16**, e1008314 (Oct. 2020).
46. Van Hoek, P., Van Dijken, J. P. & Pronk, J. T. Effect of Specific Growth Rate on Fermentative Capacity of Baker's Yeast. *Appl Environ Microbiol* **64**, 4226–4233 (Nov. 1998).
47. Mortimer, R. K. & Johnston, J. R. Life Span of Individual Yeast Cells. *Nature* **183**, 1751–1752 (June 1959).
48. Liu, P. & Acar, M. The generational scalability of single-cell replicative aging. *Sci. Adv.* **4**, eaao4666 (Jan. 2018).
49. Kaya, A. *et al.* Evolution of natural lifespan variation and molecular strategies of extended lifespan in yeast. *eLife* **10**, e64860 (Nov. 2021).
50. Henderson, K. A. & Gottschling, D. E. A mother's sacrifice: what is she keeping for herself? *Current Opinion in Cell Biology* **20**, 723–728 (Dec. 2008).
51. Steinkraus, K., Kaeberlein, M. & Kennedy, B. Replicative Aging in Yeast: The Means to the End. *Annu. Rev. Cell Dev. Biol.* **24**, 29–54 (Nov. 2008).
52. Sun, Y., Yu, R., Guo, H.-B., Qin, H. & Dang, W. A quantitative yeast aging proteomics analysis reveals novel aging regulators. *GeroScience* (July 2021).
53. Morlot, S. *et al.* Excessive rDNA Transcription Drives the Disruption in Nuclear Homeostasis during Entry into Senescence in Budding Yeast. *Cell Reports* **28**, 408–422.e4 (July 2019).
54. Fabrizio, P., Pletcher, S., Minois, N., Vaupel, J. & Longo, V. Chronological aging-independent replicative life span regulation by Msn2/Msn4 and Sod2 in *Saccharomyces cerevisiae*. *FEBS Letters* **557**, 136–142 (Jan. 2004).
55. Kaeberlein, M. Regulation of Yeast Replicative Life Span by TOR and Sch9 in Response to Nutrients. *Science* **310**, 1193–1196 (Nov. 2005).
56. Famili, I., Forster, J., Nielsen, J. & Palsson, B. O. *Saccharomyces cerevisiae* phenotypes can be predicted by using constraint-based analysis of a genome-scale reconstructed metabolic network. *Proceedings of the National Academy of Sciences* **100**, 13134–13139 (Nov. 2003).
57. Unlu, E. S. & Koc, A. Effects of Deleting Mitochondrial Antioxidant Genes on Life Span. *Annals of the New York Academy of Sciences* **1100**, 505–509 (Apr. 2007).
58. Hacioglu, E., Esmer, I., Fomenko, D. E., Gladyshev, V. N. & Koc, A. The roles of thiol oxidoreductases in yeast replicative aging. *Mechanisms of Ageing and Development* **131**, 692–699 (Nov. 2010).
59. Pirt, S. J. The maintenance energy of bacteria in growing cultures — Proceedings of the Royal Society of London. Series B. Biological Sciences (1965).
60. Van Bodegom, P. Microbial Maintenance: A Critical Review on Its Quantification. *Microbial Ecology* **53**, 513–523 (May 2007).
61. Calabrese, L. *et al.* *Role of protein degradation in growth laws* tech. rep. Company: Cold Spring Harbor Laboratory Distributor: Cold Spring Harbor Laboratory Label: Cold Spring Harbor Laboratory Section: New Results Type: article (Dec. 2021), 2021.03.25.436692.
62. Kempes, C. P. *et al.* Drivers of Bacterial Maintenance and Minimal Energy Requirements. *Frontiers in Microbiology* **8** (2017).
63. Huberts, D. H. E. W., Niebel, B. & Heinemann, M. A flux-sensing mechanism could regulate the switch between respiration and fermentation. *FEMS Yeast Research* **12**, 118–128 (Mar. 2012).
64. Dawes, I. W. & Perrone, G. G. Stress and ageing in yeast. *FEMS Yeast Research* **20**, foz085 (Feb. 2020).
65. Eleutherio, E. *et al.* Oxidative stress and aging: Learning from yeast lessons. *Fungal Biology. Biology of Fungal Systems under Stress* **122**, 514–525 (June 2018).
66. Eigenfeld, M., Kerpes, R. & Becker, T. Understanding the Impact of Industrial Stress Conditions on Replicative Aging in *Saccharomyces cerevisiae*. *Frontiers in Fungal Biology* **2** (2021).

67. Chandrasekaran, S. & Price, N. D. Probabilistic integrative modeling of genome-scale metabolic and regulatory networks in *Escherichia coli* and *Mycobacterium tuberculosis*. *Proc Natl Acad Sci USA* **107**, 17845–17850 (Oct. 2010).
68. Monteiro, P. T. *et al.* YEASTRACT+: a portal for cross-species comparative genomics of transcription regulation in yeasts. *Nucleic Acids Research* **48**, D642–D649 (Jan. 2020).
69. Kanti Das, T., Wati, M. R. & Fatima-Shad, K. Oxidative Stress Gated by Fenton and Haber Weiss Reactions and Its Association With Alzheimer’s Disease. *Arch Neurosci* **2** (Aug. 2014).
70. Cobley, J. N. Mechanisms of Mitochondrial ROS Production in Assisted Reproduction: The Known, the Unknown, and the Intriguing. *Antioxidants* **9**, 933 (Sept. 2020).
71. Kuge, S. & Jones, N. YAP1 dependent activation of TRX2 is essential for the response of *Saccharomyces cerevisiae* to oxidative stress by hydroperoxides. *The EMBO Journal* **13**, 655–664 (Feb. 1994).
72. Kuge, S., Toda, T., Iizuka, N. & Nomoto, A. Crm1 (XpoI) dependent nuclear export of the budding yeast transcription factor yAP-1 is sensitive to oxidative stress. *Genes to Cells* **3**, 521–532 (Aug. 1998).
73. Delaunay, A., Pflieger, D., Barrault, M.-B., Vinh, J. & Toledano, M. B. A Thiol Peroxidase Is an H₂O₂ Receptor and Redox-Transducer in Gene Activation. *Cell* **111**, 471–481 (Nov. 2002).
74. Veal, E. A., Ross, S. J., Malakasi, P., Peacock, E. & Morgan, B. A. Ybp1 Is Required for the Hydrogen Peroxide-induced Oxidation of the Yap1 Transcription Factor. *Journal of Biological Chemistry* **278**, 30896–30904 (Aug. 2003).
75. Isoyama, T., Murayama, A., Nomoto, A. & Kuge, S. Nuclear Import of the Yeast AP-1-like Transcription Factor Yap1p Is Mediated by Transport Receptor Pse1p, and This Import Step Is Not Affected by Oxidative Stress. *Journal of Biological Chemistry* **276**, 21863–21869 (June 2001).
76. Moye-Rowley, W. S. Transcription Factors Regulating the Response to Oxidative Stress in Yeast. *Antioxidants & Redox Signaling* **4**, 123–140 (Feb. 2002).
77. Izawa, S. *et al.* Thioredoxin Deficiency Causes the Constitutive Activation of Yap1, an AP-1-like Transcription Factor in *Saccharomyces cerevisiae*. *Journal of Biological Chemistry* **274**, 28459–28465 (Oct. 1999).
78. Grant, C. M., Collinson, L. P., Roe, J.-H. & Dawes, I. W. Yeast glutathione reductase is required for protection against oxidative stress and is a target gene for yAP-1 transcriptional regulation. *Molecular Microbiology* **21**, 171–179 (July 1996).
79. Dumond, H., Danielou, N., Pinto, M. & Bolotin-Fukuhara, M. A large-scale study of Yap1p-dependent genes in normal aerobic and H₂O₂-stress conditions: the role of Yap1p in cell proliferation control in yeast. *Mol Microbiol* **36**, 830–845 (May 2000).
80. Xu, Q., Porter, S. W. & West, A. H. The Yeast YPD1/SLN1 Complex. *Structure* **11**, 1569–1581 (Dec. 2003).
81. Singh, K. K. The *Saccharomyces cerevisiae* sln1p-ssk1p two-component system mediates response to oxidative stress and in an oxidant-specific fashion. *Free Radical Biology and Medicine* **29**, 1043–1050 (Nov. 2000).
82. Morgan, B. A. The Skn7 response regulator controls gene expression in the oxidative stress response of the budding yeast *Saccharomyces cerevisiae*. *The EMBO Journal* **16**, 1035–1044 (Mar. 1997).
83. Charizanis, C., Juhnke, H., Krems, B. & Entian, K.-D. The oxidative stress response mediated via Pos9/Skn7 is negatively regulated by the Ras/PKA pathway in *Saccharomyces cerevisiae*. *Mol Gen Genet* **261**, 740–752 (June 1999).
84. Hasan, R. *et al.* The control of the yeast H₂O₂ response by the Msn2/4 transcription factors. *Mol Microbiol* **45**, 233–241 (July 2002).
85. Boissnard, S. *et al.* H₂O₂ Activates the Nuclear Localization of Msn2 and Maf1 through Thioredoxins in *Saccharomyces cerevisiae*. *Eukaryot Cell* **8**, 1429–1438 (Sept. 2009).
86. Lee, J. *et al.* Yap1 and Skn7 Control Two Specialized Oxidative Stress Response Regulons in Yeast. *Journal of Biological Chemistry* **274**, 16040–16046 (June 1999).

87. Bezanson, J., Edelman, A., Karpinski, S. & Shah, V. B. Julia: A Fresh Approach to Numerical Computing. *SIAM Rev.* **59**, 65–98 (Jan. 2017).
88. Funahashi, A., Morohashi, M., Kitano, H. & Tanimura, N. CellDesigner: a process diagram editor for gene-regulatory and biochemical networks. *BIOSILICO* **1**, 159–162 (Nov. 2003).

Figures

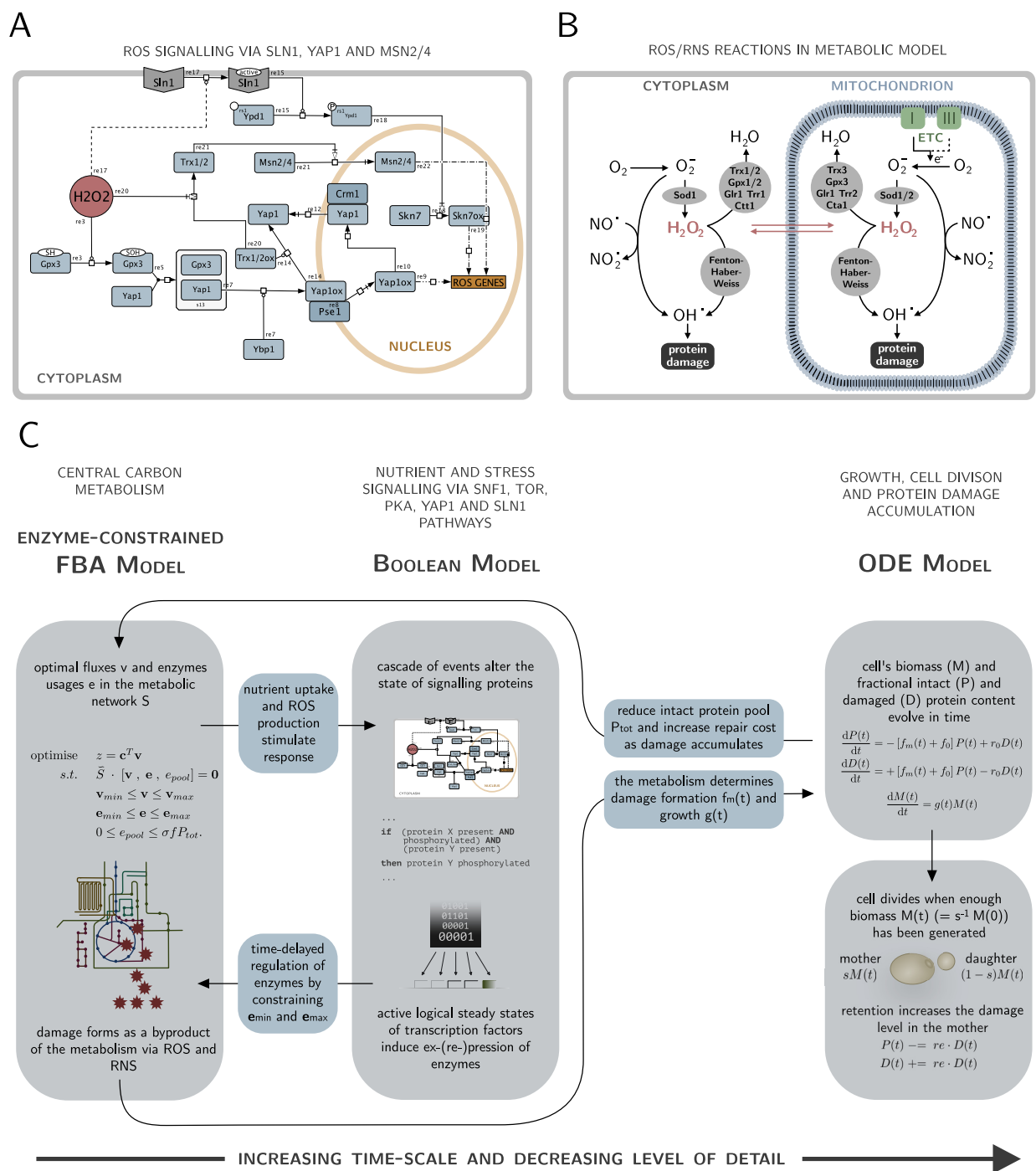


Figure 1: Multi-scale model construction (A) Yap1 and Sln1 signalling in response to oxidative stress via H_2O_2 . The two pathways were added to Boolean signalling network. Trx1/2 exhibits cross-talk to Msn2/4, a component that is also part of the nutrient sensing pathway PKA. The figure is made with Cell Designer [88]. (B) ROS/RNS reactions that were added to the enzyme-constrained FBA model. The cell is exposed to oxidative stress as a consequence of electron leakage in the electron transport chain (ETC). (C) Schematic view of one time step in the multi-scale model. The enzyme-constrained FBA fluxes based on the current fraction of intact and damaged proteins determine the input states of the Boolean signalling layer. A set of Boolean rules alter the states of the signalling proteins, that eventually induce gene ex-/repression via a transcriptional layer, leading to constraints in individual enzyme usages. Solving the regulated enzyme-constrained FBA gives rise to a growth rate as well as a metabolic damage formation rate, that feed into the ODE model of growth and damage accumulation that is then solved for one time step. If the cell has accumulated enough biomass, the cell divides in an instantaneous event. Iterating the model over time-steps until the model becomes infeasible corresponds to a lifespan simulation.

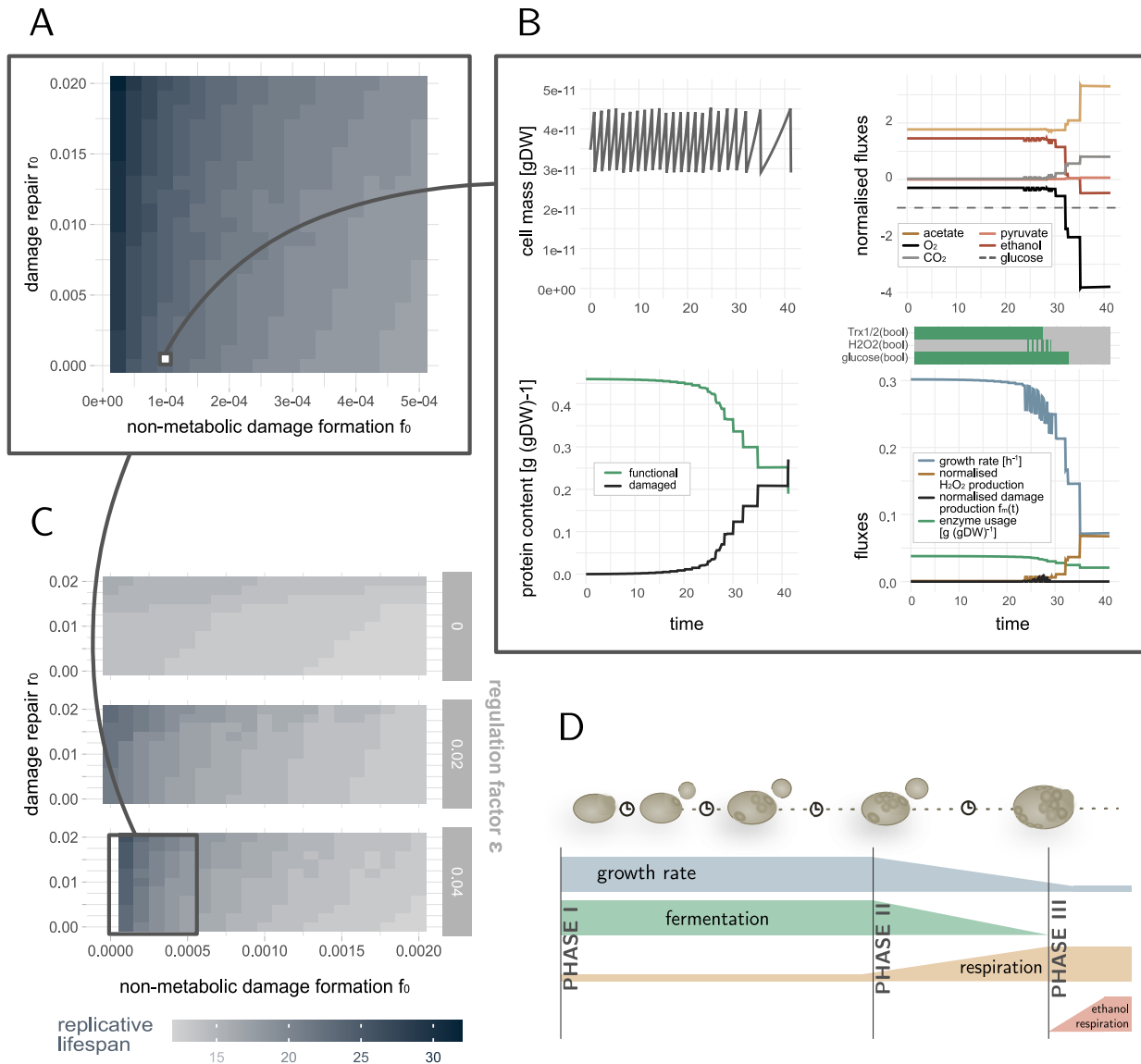


Figure 2: Lifespan simulations of yeast wildtype cells. (A) Replicative lifespans for typical yeast wildtype cells with varying damage repair r_0 and non-metabolic damage formation rates f_0 . The model reproduces 17-32 divisions. (B) Zoom into variables of all three model parts over time for a specific exemplary parameter set ($f_0 = 0.0001$, $r_0 = 0.0005$): cell mass, fraction of intact and damaged proteins, growth rate, exchange fluxes normalised by the glucose uptake rate (dashed black line) in the metabolic model (> 0 : production rates, < 0 : uptake rates), functional enzyme pool and input signals received by the signalling network (green: present, grey: not present). As cells age they accumulate damage, the growth rate drops and the metabolism needs to adapt. (C) Zoom out for varying damage repair r_0 and non-metabolic damage formation rates f_0 and regulation factors ϵ . If the tile is not filled ($f_0 = 0.0$ and $\epsilon = 0.04$), the simulated cell did not stop dividing in the simulation time. Stronger regulation increases the replicative lifespan and wildtype cells with more than 22 divisions cannot be achieved in this resolution if the regulation factor $\epsilon < 0.4$. (D) Schematic view of the metabolic phases a cells undergoes during its replicative life: from maximal growth and fermentation (I) it slowly switches to respiration when the growth rate drops (II) until it eventually can also take up ethanol to produce energy close to cell death (III).

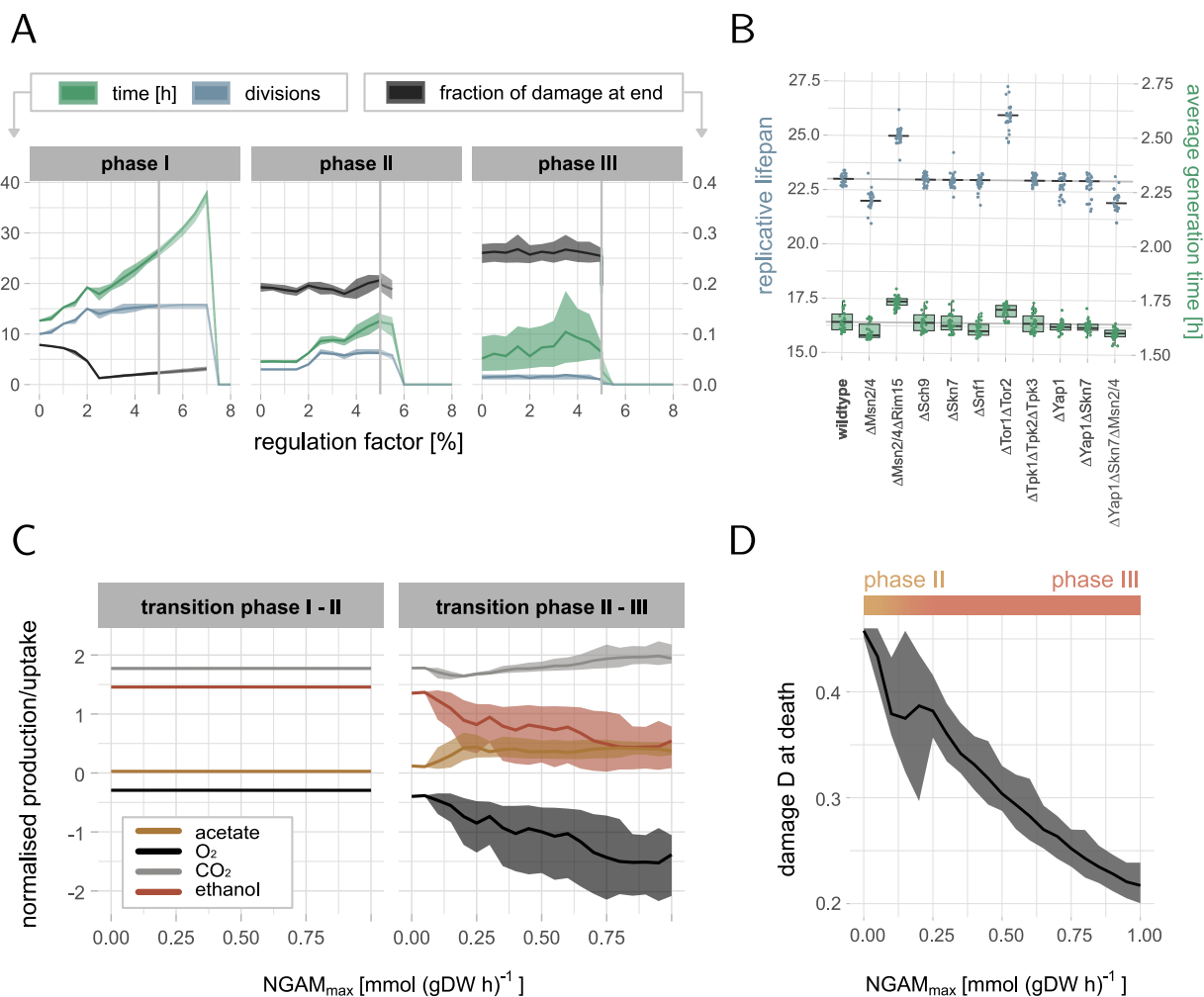


Figure 3: Effect of regulation and NGAM on lifespan All distributions are based on 29 wildtype parameter sets with $f_0 \leq 5 \cdot 10^{-4}$ and $r_0 \leq 2 \cdot 10^{-2}$ that lead to 23 divisions (from data in Fig 2A). (A) Effect of the regulation factor ϵ , i.e. how strong gene expression changes caused by stress signalling affect the metabolic model, on the lifespan simulations (line: mean, ribbons: 5% and 95% quantiles). Our model can only handle $\epsilon \leq 5\%$. Weak regulation $\epsilon \leq 2.5\%$ mostly affects phase I, and stronger regulation $\epsilon > 2.5\%$ phase II. (B) Distributions of replicative lifespans and average generation times for cells with knockouts of signalling proteins in the different pathways of the Boolean model (line: median, box: IQR, whiskers: median ± 1.5 IQR). (C) Effect of the age-dependent non-growth associated maintenance NGAM (Eq (5)) on the transition between the phases (line: mean, ribbons: 5% and 95% quantiles). Increasing cost for non-growth associated maintenance, such as damage repair, can explain the switch from fermentation to respiration in phase II, indicated by higher O_2 uptake, lower ethanol and higher CO_2 and acetate production. The fluxes are normalised by the glucose uptake rate, negative fluxes are uptake and positive production rates. (D) Damage at cell death depending on NGAM (line: mean, ribbons: 5% and 95% quantiles). Increasing NGAM leads to lower damage tolerance before cell death, that happens in phase II for low NGAM and in phase III for higher NGAM.

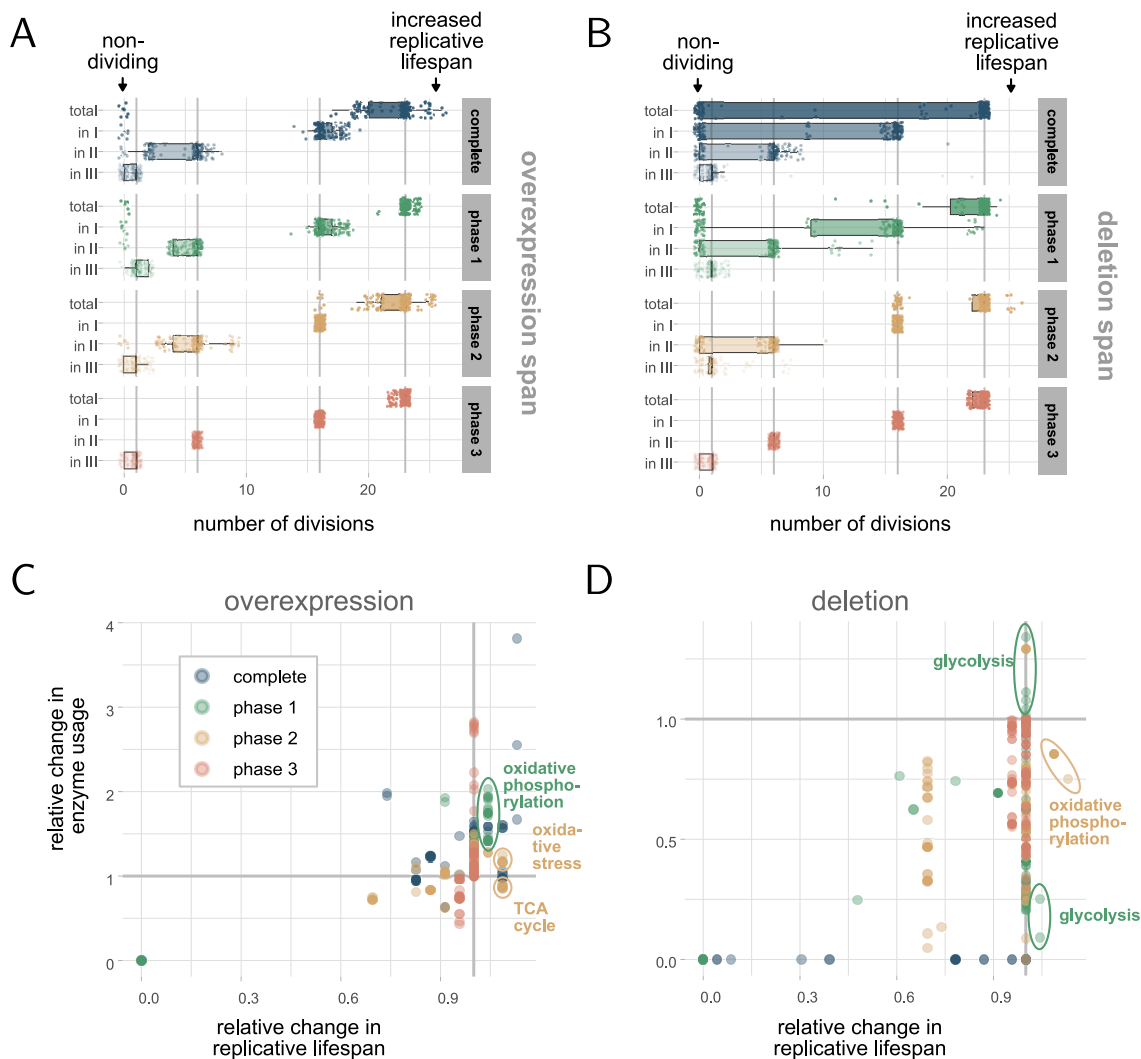


Figure 4: Effect of enzyme perturbations on lifespan The simulations are based on $f_0 = 0.0001$ and $r_0 = 0.0005$ (as in Fig 2B) and perturbations (deletion or overexpression) in individual enzymes or isoenzyme combinations (140 + 23 cases) for different phases in the metabolic model. (A-B) Distribution (line: median, box: IQR, whiskers: median ± 1.5 IQR) of the number of divisions in total and in particular phases upon overexpression or deletion of enzymes during specific times (facets) in relation to the wildtype (grey lines). An intervention in a specific phase can have a different effect than an intervention over the whole lifespan. (C-D) Relation between replicative lifespan and total enzyme usage relative to the wildtype. Each dot represents one simulation with the perturbation in a specific phase of an enzyme/isoenzymes. Both enzyme deletion and overexpression can lead to an increased but also decreased total usage of the enzyme compared to the wildtype.